Exploring common genetic contributors to neuroprotection from amyloid pathology

Mabel Seto[a,b,c], Emily R. Mahoney[a,b,d], Logan Dumitrescu[a,b,d], Vijay K Ramanan[l], Corinne D. Engelman[e,f], Yuetiva Deming[e,f], Marilyn Albert[g], Sterling C. Johnson[f], Henrik Zetterberg[h,i,j,k], Kaj Blennow[h,i], Prashanthi Vemuri[m], Angela L. Jefferson[a,d], Timothy J. Hohman[a,b,c,d,#] for the Alzheimer's Disease Neuroimaging Initiative*

[a]*Vanderbilt Memory and Alzheimer's Center, Vanderbilt University Medical Center, Nashville, TN, USA*

[b]*Vanderbilt Genetics Institute, Vanderbilt University Medical Center, Nashville, TN, USA*

[c]*Department of Neurology, Vanderbilt University Medical Center, Nashville, TN, USA*

[d]*Department of Pharmacology, Vanderbilt University, Nashville, TN, USA*

[e]*Department of Population Health Sciences, University of Wisconsin, School of Medicine and Public Health, Madison, WI, USA*

[f]*Alzheimer's Disease Research Center, University of Wisconsin School of Medicine and Public Health, Madison, WI and Geriatric Education and Clinical Center, Wm. S. Middleton VA Hospital, Madison, WI, USA*

[g]*Department of Neurology, the Johns Hopkins University School of Medicine, Baltimore, MD, USA*

[h]*Department of Psychiatry and Neurochemistry, Institute of Neuroscience and Physiology, The Sahlgrenska Academy at University of Gothenburg, Mölndal, Sweden*

[i]*Clinical Neurochemistry Laboratory, Sahlgrenska University Hospital, Mölndal, Sweden*

[j]*Department of Neurodegenerative Disease, UCL Institute of Neurology, London, United Kingdom*

[k]*UK Dementia Research Institute at UCL, London, United Kingdom*

[l]*Department, of Neurology, Mayo Clinic, Rochester, MN, USA*

[m]*Department of Radiology, Mayo Clinic, Rochester, MN, USA*

**Data used in preparation of this article were obtained from the Alzheimer's Disease Neuroimaging Initiative (ADNI) database (adni.loni.usc.edu). As such, the investigators within the ADNI contributed to the design and implementation of ADNI and/or provided data but did not participate in analysis or writing of this report. A complete listing of ADNI investigators can be found at: http://adni.loni.usc.edu/wp-content/uploads/how_to_apply/ADNI_Acknowledgement_List.pdf*

[#]Address Correspondence to:
Timothy J Hohman, Ph.D.
Vanderbilt Memory & Alzheimer's Center
Vanderbilt University Medical Center
1207 17th Ave S
Nashville, TN 37212, USA
Phone: 615–343–8429
Email: Timothy.J.Hohman@vumc.org

ABSTRACT

Preclinical Alzheimer's disease describes some individuals who harbor Alzheimer's pathologies but are asymptomatic. For this study, we hypothesized that genetic variation may help protect some individuals from Alzheimer's-related neurodegeneration. We therefore conducted a genome-wide association study using 5,891,064 common variants to assess whether genetic variation modifies the association between baseline beta-amyloid, as measured by both cerebrospinal fluid and positron emission tomography, and neurodegeneration defined using MRI measures of hippocampal volume.

We combined and jointly analyzed genotype, biomarker, and neuroimaging data from non-Hispanic white individuals who were enrolled in four longitudinal aging studies (n=1065). Using regression models, we examined the interaction between common genetic variants (Minor Allele Frequency > 0.01), including *APOE*-ε4 and *APOE*-ε2, and baseline cerebrospinal levels of amyloid (CSF Aβ42) on baseline hippocampal volume and the longitudinal rate of hippocampal atrophy. For targeted replication of top findings, we analyzed an independent dataset (n=808) where amyloid burden was assessed by Pittsburgh Compound B ([^{11}C]-PiB) PET.

In this study, we found that *APOE*-ε4 modified the association between baseline CSF Aβ42 and hippocampal volume such that *APOE*-ε4 carriers showed more rapid atrophy, particularly in the presence of enhanced amyloidosis. We also identified a novel locus on chromosome 3 that interacted with baseline CSF Aβ42. Minor allele carriers of rs62263260, an expression quantitative trait locus for the *SEMA5B* gene, ($p=1.46\times10^{-8}$; 3:122675327) had more rapid neurodegeneration when amyloid burden was high and slower neurodegeneration when amyloid was low. The rs62263260 x amyloid interaction on longitudinal change in hippocampal volume was replicated in an independent dataset (p=0.0112) where amyloid burden was assessed by PET.

In addition to supporting the established interaction between *APOE* and amyloid on neurodegeneration, our study identifies a novel locus that modifies the association between beta-amyloid and hippocampal atrophy. Annotation results may implicate *SEMA5B*, a gene involved in synaptic pruning and axonal guidance, as a high-quality candidate for functional confirmation and future mechanistic analysis.

Key Words: Alzheimer's, amyloid, genetics, hippocampus

Abbreviations: ADNI, Alzheimer's Disease Neuroimaging Initiative; AMP-AD, Accelerating Medicines Partnership Program for Alzheimer's; APOE, apolipoprotein E; beta-amyloid, Aβ, Aβ42; BIOCARD, Biomarkers of Cognitive Decline Among Normal Individuals; CSF, cerebrospinal fluid; eQTL, expression quantitative trait locus; FDR, false discovery rate; GMM, Gaussian mixture model; GO, Gene Ontology; GWAS, genome wide association study; GTEx, NIH Genotype-Tissue Expression Portal; ICV, intracranial volume; LD, linkage disequilibrium; MCSA, Mayo Clinic Study of Aging; mQTL, methylation quantitative trait locus; MCI, mild cognitive impairment; MAF, minor allele frequency; MRI, magnetic resonance imaging; PheWAS, phenome-wide association study; PET, positron emission tomography; PC, principal component; QC, quality control; SNP, single nucleotide polymorphism; SUVR, standardized uptake value ratio; VMAP, Vanderbilt Memory and Aging Project; WRAP, Wisconsin Registry for Alzheimer's Prevention

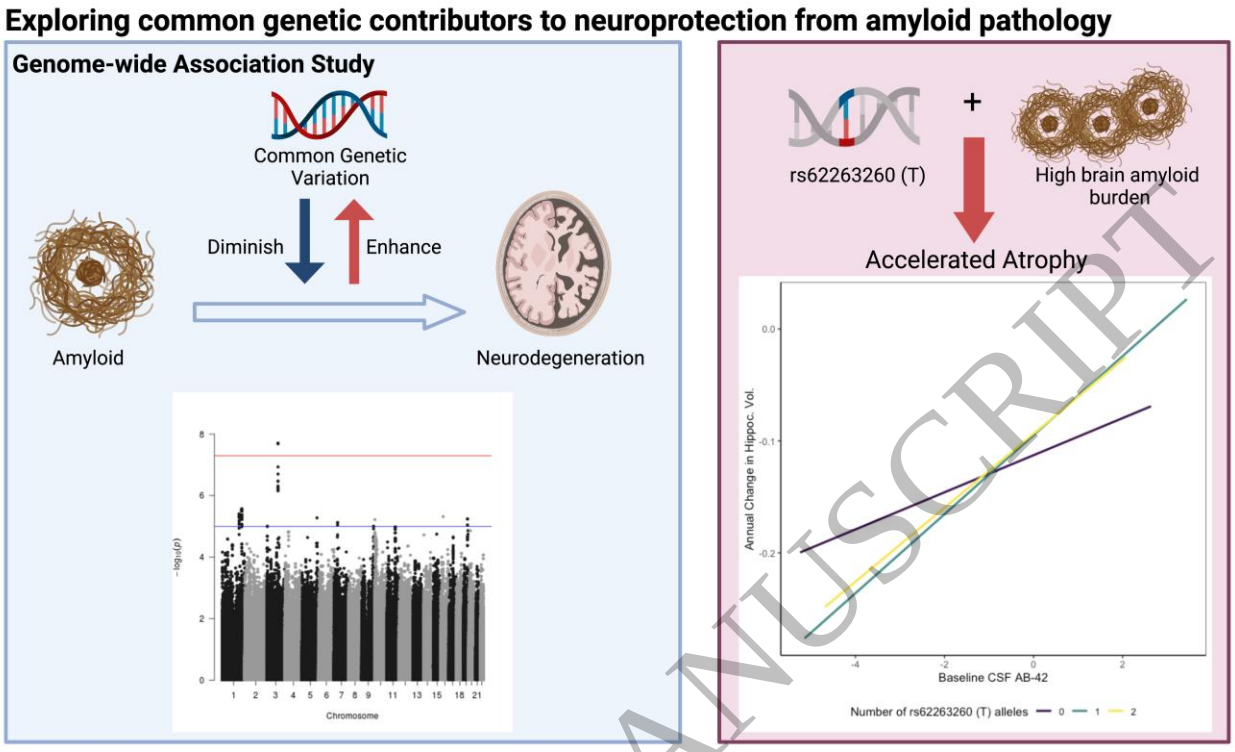

Graphical Abstract
165x100 mm (1.6 x DPI)

INTRODUCTION

The genomic and phenotypic complexity of Alzheimer's disease has resulted in a challenging therapeutic landscape including numerous high-profile clinical trial failures and no disease-modifying therapies. Few novel targets have been identified and pursued for Alzheimer's drug discovery, resulting in the slowed discovery and stalled development of effective treatments.[1-4] However, recent studies suggest that the exploration of biological mechanisms behind Alzheimer's disease from a different perspective may allow for new opportunities in Alzheimer's drug discovery to arise.

Asymptomatic Alzheimer's disease, or preclinical Alzheimer's disease, is a phenomenon in which individuals present with the neuropathological hallmarks of Alzheimer's, but do not yet show clinical signs of cognitive impairment.[5-7] Some of these individuals may prove to be resilient. Modifiable risk

factors that contribute to resilience have been a major focus of the field, including factors like educational attainment that have been leveraged as proxy measures in classical cognitive reserve literature.[8] Resilience has also been defined in two parts: better than expected cognitive function given the overall level of Alzheimer's disease pathologies (*i.e.*, cognitive resilience) and less than expected brain atrophy given the level of Alzheimer's pathologies (*i.e.,* brain resilience).[9] While modifiable lifestyle factors certainly contribute to such resilience,[10, 11] there is also emerging evidence from our group and others' that resilience is heritable and may have a genetic basis.[12-16]

One notable example is the apolipoprotein E (*APOE*) polymorphic alleles, as *APOE*-ε2 allele carriers have reduced Alzheimer's disease risk.[17-19] In addition, recent studies have suggested that the genetic architecture of resilience is distinct from that of clinical Alzheimer's disease with only a small contribution of *APOE,*[20] suggesting that uncovering the genetic architecture of resilience may provide new insight into genomic pathways of protection.

The present analytical approach will further probe the genetic basis of resilience by identifying common genetic variants that modify the association between baseline amyloid deposition and future neurodegeneration.[21-26] For this study, we will leverage both cerebrospinal fluid (CSF) and positron emission tomography (PET) biomarkers of amyloid-β as well as longitudinal hippocampal volume measured with magnetic resonance imaging (MRI) as our proxy measure of neurodegeneration.[27]

MATERIALS AND METHODS

Participants

Data for mega-analysis were acquired from four longitudinal studies of aging and Alzheimer's disease that include CSF biomarkers of Alzheimer's neuropathology, genotype data, and neuroimaging. The studies are as follows: the Alzheimer's Disease Neuroimaging Initiative (ADNI), Vanderbilt Memory

and Aging Project (VMAP), Wisconsin Registry for Alzheimer's Prevention (WRAP), and the Biomarkers of Cognitive Decline Among Normal Individuals (BIOCARD) study. Data from the Mayo Clinic Study of Aging (MCSA) was used for replication. Additional information for each study can be found in the **Supplementary Methods**.

Genotyping and Quality Control Procedures

Genotyping was performed by each study on different genotyping platforms (see **Supplementary Table 1**). Genotyping data were limited to non-Hispanic white individuals whose principal components (PCs) overlayed with individuals of European ancestry using the 1000 Genomes CEU reference panel. Quality control (QC) was performed on genotype data from each cohort separately using PLINK software (version 1.9b_5.2).[28] Before imputation, single nucleotide polymorphisms (SNPs) with genotyping efficiency <95%, minor allele frequency (MAF) <1%, or deviation from Hardy-Weinberg equilibrium ($p<1x10^{-6}$) were excluded. Furthermore, we excluded participants whose call rate was <99%, who exhibited an inconsistency between reported and genetic sex, or who exhibited excess relatedness (PI_HAT>0.25). We also removed individuals who were outliers based on their ancestral PCs (calculated with EIGENSOFT version 7.2.1)[29] or who were statistical outliers in heterozygosity rate (>5 SD).

Imputation was performed on the Michigan Imputation Server[30] using the HRC r1.1.2016 reference panel (Build 37) and SHAPEIT phasing. Imputed genetic data were further filtered for imputation quality ($r^2>0.9$) and biallelic SNPs. To create the joint dataset, we merged genotype data from ADNI, VMAP, WRAP, and BIOCARD, excluding multiallelic SNPs, duplicate SNPs, SNPs that were not present in all datasets, and SNPs with genotyping efficiency <99%. Additional participants were excluded for relatedness or outlying PCs, resulting in a dataset consisting of 1065 individuals and 5,891,064 variants.

MCSA GWAS Data Acquisition, QC, and Imputation

MCSA GWAS QC procedures are included in **Supplementary Methods** and described previously.[31]

Hippocampal Volume Standardization and Slope Calculation

MRI was performed at each study site; acquisition and processing protocols are described elsewhere (**Supplementary Table 2**).[32-35] We excluded images that failed visual QC, that were taken >90 days prior to CSF acquisition, or that were statistical outliers (>5 SD).

Total hippocampal volume was harmonized across studies using a two-step procedure, and the standardization of all hippocampal volume measurements were based on the first MRI scan of cognitively normal participants at baseline. First, raw hippocampal volume measurements were adjusted to remove the effects of sex and intracranial volume (ICV; see **Supplementary Methods**). Second, we calculated Z-scores using the mean and standard deviation (SD) of the adjusted volume from cognitively normal participants at baseline, resulting in our standardized hippocampal volume variable (**Supplementary Figure 1**). Data from ADNI1 and ADNI2 were harmonized separately to account for differences in scanner strength (1.5T vs 3T).

MCSA MRI

MRI for MCSA participants was acquired on 3T scanners (General Electric Healthcare, Waukesha, WI, USA) using protocols aligned with ADNI.[36] Information for acquisition and processing has been described elsewhere.[37-39] Hippocampal volume and ICV were derived using FreeSurfer (version 5.3).

CSF Biomarker Standardization

CSF concentration of the 42 amino acid-long amyloid β form (Aβ42) was acquired via lumbar puncture and quantification by immunoassay performed by each longitudinal aging study. Acquisition and quantification protocols have been reported by each study.[33-35, 40]

CSF Aβ42 was harmonized using a two-component Gaussian mixture model (GMM).[41] The mean and SD estimated from the model-predicted low amyloid gaussian distribution in cognitively normal individuals was used to standardize all values (**Supplementary Figure 2A**) as previously described.[41-43]

Amyloid Positron Emission Tomography

To support our findings, we leveraged amyloid PET data from MCSA participants measured with Pittsburgh compound B ([^{11}C]-PiB), as described elsewhere.[44, 45]

We also examined amyloid PET data from ADNI measured with Pittsburgh compound B ([^{11}C]-PiB) and florbetapir ([^{18}F]-AV-45). Additional details on acquisition and pre- and post-processing pipelines can be found on the ADNI website (www.adni-info.org). Mean standardized uptake value ratio (SUVR) values were standardized using a similar two-component GMM as aforementioned, following previously published methods (**Supplementary Figure 2B**).[41, 46]

Statistical Analyses

Genome-wide association analyses (GWAS) were conducted using the joint dataset (see above) with PLINK and R (version 3.6.0). Both baseline hippocampal volume and annual change in hippocampal volume were used as continuous outcomes. The annual change in hippocampal volume was determined using linear mixed-effects regression, where the intercept and slope (time from baseline MRI scan) were entered as both fixed and random effects. Covariates for the GWAS included age at first MRI, sex, and the first three ancestral PCs (calculated using EIGENSOFT version 7.2.1)[29] to account for unmeasured

population stratification. For computational efficiency, we extracted the hippocampal volume slopes from mixed-effects regression models and entered them as continuous outcomes in a linear regression with PLINK. The interaction term between each SNP and continuous CSF Aβ42 was used to identify variants that modified the association between Aβ42 and annual change in hippocampal volume. All variants were tested using additive coding. Genome-wide significance was set *a priori* to $p<5x10^{-8}$.[47] Although this linear regression approach was more computationally feasible, the full linear mixed-effects model has multiple advantages including the estimation of both intercepts and slopes in the same model. For that reason, we did run the full linear-mixed effects model for all variants meeting suggestive significance ($p<1x10^{-5}$) to ensure our results are not driven by the two-stage analytical approach (**Supplementary Table 3**) and to have a model that aligns with the linear mixed-effects model used in our independent replication. Sensitivity analyses included *APOE*-ε4 allele count, MRI scanner strength, and a variable for cohort as additional covariates. Additional sensitivity analyses include stratifying by diagnosis, aging study, and adding a cohort x age interaction term (**Supplementary Tables 4, 5**).

To validate the candidate locus discovered in our primary analyses, we also tested the target SNP, rs62263260, using additive coding in the independent dataset from MCSA (n=808). Replication analyses used a mixed-effects linear regression to examine the SNP interaction with baseline amyloid PET standardized uptake value ratio (SUVR), against longitudinal hippocampal volume as the outcome and including age, sex, and ICV as covariates. In this model, ICV was included as an additional covariate because hippocampal volume measurements were not adjusted for the effect of ICV in MSCA.

We also leveraged amyloid PET data from ADNI (n=667) testing the SNP interaction with standardized mean SUVR on the same hippocampal outcome. Covariates included age, sex, and PET

tracer. Both linear and linear mixed-effects regression models were used. Harmonization across tracers was completed leveraging a GMM as previously published.[48]

Finally, we used a linear regression model to assess the interaction between *APOE* allele count (ε4 additive coding and ε2 dominant coding due to few homozygous carriers) with CSF amyloid on cross-sectional and longitudinal hippocampal volume (n=1537, **Supplementary Table 6**).

Functional Annotation

Expression quantitative trait locus (eQTL) annotation was performed using the NIH Genotype-Tissue Expression (GTEx) Portal[49] and brain cortex eQTL data from Sieberts et al. When assessing eQTL p-values for the 44 available tissues within GTEx, we performed Bonferroni correction to account for multiple comparisons (significant p<0.0011). Additional annotation leveraged both INFERNO (http://inferno.lisanwanglab.org/) and the Brain xQTL Serve database (http://mostafavilab.stat.ubc.ca/xqtl/).

Colocalization Analysis

To examine genes in the region of the significant locus, we performed colocalization analysis using summary statistics from the SNP x CSF Aβ42 GWAS and brain cortex eQTL data from Sieberts et al., (*i.e.*, dorsolateral prefrontal cortex, temporal cortex)[50] as well as eQTL data from GTEx v8 (*i.e.*, tissues where rs62263260 was a statistically significant eQTL for any gene: esophagus muscularis, testis, brain anterior cingulate cortex BA24). Using coloc (version 3.2-1)[51, 52], we performed colocalization in a 1Mb window around the lead SNP, rs62263260 with default priors.[52] All protein coding genes within that window (Chromosome 3, 123175327: 122175327) were tested (**Supplementary Table 7**). A posterior probability greater than 80% (PP4 > 0.8) is indicative of colocalization.[51, 52]

Post-hoc *SEMA5B* Analyses

To assess whether *SEMA5B* expression differs by AD diagnosis, we utilized summaries of case/control analyses from the Accelerating Medicines Partnership Program for Alzheimer's (AMP-AD). Data from this project are made freely available online (https://agora.adknowledgeportal.org).

Furthermore, we examined neuronal *SEMA5B* expression data. Pyramidal neuron expression data for these analyses was obtained from the NIH Gene Expression Omnibus (https://www.ncbi.nlm.nih.gov/geo/). Additional details on brain collection, expression profiling, and microarray analysis are described elsewhere.[53-56] Tissues include the entorhinal cortex, hippocampus, medial temporal gyrus, posterior cingulate cortex, primary visual cortex, and superior frontal gyrus.

Repeated measures ANOVA was used to evaluate differences in *SEMA5B* expression in AD patients compared to controls across brain regions. Covariates included age, sex, and brain region. Post-hoc paired comparisons within each region were performed leveraging independent samples t-tests (one-tailed). We corrected for multiple comparisons leveraging the Bonferroni procedure for the six brain regions evaluated.

MAGMA Pathway Analysis

Gene and pathway analyses were conducted using MAGMA version 1.08.[57] Gene test analyses used the SNP-wise mean model specified in MAGMA. Results were corrected for multiple comparisons using the false-discovery rate (FDR) procedure. Gene set consortia are described in **Supplementary Methods**.

Data Availability

Data from the ADNI study are shared through the LONI Image and Data Archive (https://ida.loni.usc.edu/). Data from BIOCARD can be requested at https://www.biocard-se.org/. Data

from WRAP can be requested at https://wrap.wisc.edu/data-requests/. The Sieberts et al., 2020 brain cortex eQTL data was obtained through the AMP-AD Knowledge Portal.[50] Additional data sharing will be facilitated by the individual cohort study groups.

RESULTS

Participant characteristics are presented in **Table 1**. We observed statistically significant differences between participants in each diagnostic category as expected except for the average number of follow-up visits. Participants in the BIOCARD and WRAP studies are younger than those enrolled in ADNI and VMAP (**Supplementary Table 8**). Additionally, ADNI includes more participants that have been diagnosed with MCI and Alzheimer's disease than in VMAP, WRAP, or BIOCARD.

Using the composite dataset, we performed GWAS to identify common SNPs that modify the association between baseline CSF Aβ42 and baseline hippocampal volume as well as annual change in hippocampal volume. Suggestively significant loci ($p<1x10^{-5}$) are displayed in **Supplementary Tables 3, 9, and 10**. We also expand on a study by Chiang et al.[58] that explored whether *APOE*-ε4 allele status modified the association between baseline CSF amyloid and longitudinal changes in hippocampal volume.

APOE Allele Associations with Hippocampal Atrophy

APOE results are presented in **Table 2.** As expected, *APOE*-ε4 allele count was associated with lower baseline hippocampal volume (β=-0.43, $p<2x10^{-16}$) and faster atrophy (β=-0.03, $p<2x10^{-16}$). Additionally, *APOE*-ε2 carriers have greater hippocampal volume at baseline (β=0.25, p=0.02) and slower atrophy (β=0.02, p=0.0002) compared to non-carriers.

APOE Allele Interactions with Baseline CSF Aβ42

As seen previously by Chiang et al.,[58] *APOE*-ε4 significantly interacted with baseline CSF Aβ42 (β=0.11, p=0.0004, **Figure 1**) on hippocampal volume such that *APOE*-ε4 carriers with higher brain amyloid burden display lower hippocampal volumes and more rapid hippocampal atrophy. We also observe an interaction between *APOE*-ε2 and baseline CSF Aβ42 on baseline hippocampal volume, though it did not survive correction for multiple comparisons. *APOE*-ε2 did not interact with CSF Aβ42 on longitudinal change in hippocampal volume. (**Table 2, Supplementary Table 11**).

Variant Interactions with Baseline CSF A*β*42

No significant interactions with CSF Aβ42 in cross-sectional analyses were observed. In longitudinal analyses, we identified a novel genetic locus on chromosome 3 (rs62263260-T, β=0.026, $p=1.46x10^{-8}$, MAF=0.12, **Table 3, Supplementary Table 12**) that is located within an intron of the *SEMA5B* gene (**Figure 2A, B**). Among participants harboring a high baseline brain amyloid burden (*i.e.*, low CSF Aβ42 levels), minor allele (T) carriers of rs62263260 demonstrated a faster rate of hippocampal atrophy (**Figure 3A**). At lower brain amyloid levels, minor allele carriers of rs62263260 had slower rates of hippocampal atrophy. Two additional SNPs within this region reached genome-wide significance (**Table 3**) and are in high LD ($r^2>0.8$) with the index SNP, rs62263260 (**Figure 2B**). The main effect of rs62263260 was not significantly associated with longitudinal atrophy (p>0.1). Genome-wide significance of the rs62263260 x CSF Aβ42 interaction did not change when using linear-mixed effects regression (β=0.03, $p=3.13x10^{-8}$) as opposed to linear regression (**Supplementary Table 3, 13**).

Replication of rs62263260 Interaction with Amyloid Load in the Mayo Clinic Study of Aging

In the independent MCSA cohort where amyloid burden was assessed by [^{11}C]-PiB PET, rs62263260 again displayed a significant interaction with baseline brain amyloid levels to predict

longitudinal hippocampal atrophy (n=808, β=-0.24, p=0.0112). Presence of the minor (T) allele was associated with a faster rate of hippocampal atrophy among those with higher baseline amyloid burden (*i.e.,* higher levels of amyloid PET and/or lower levels of CSF amyloid), and slower rates among those with low amyloid burden validating our initial findings in the discovery dataset. Similar results to MCSA were observed when leveraging amyloid PET data from ADNI (n=667; β=-0.0055, p=0.0045; **Supplementary Figure 3**). Linear mixed-effects regression results (β=-0.013, p=0.013) were largely consistent with the aforementioned PET results in ADNI.

Sensitivity Analyses

The rs62263260 x amyloid interaction results maintained genome-wide significance in sensitivity analyses covarying for age, sex, PC1-3, *APOE*-ε4, and scanner strength (**Supplementary Table 13**). When covarying for age, sex, PC1-3, and study, the significance becomes slightly attenuated ($p=7.7x10^{-8}$).

Functional Annotation of Significant SNPs

The index SNP rs62263260, is a significant eQTL for the *SEMA5B* gene in the brain with associations in other tissues including the esophagus (**Figure 3B**). In addition, carriers of the minor allele (T) appear to have higher levels of *SEMA5B* expression compared to non-carriers (**Supplementary Figure 4,** eQTL information from Sieberts et al., 2020). To determine whether *SEMA5B* was the acting gene in the region, colocalization analysis was performed. rs62263260 strongly colocalized with *SEMA5B* expression in the esophagus muscularis in GTEx v8 (PP4 > 0.99). In other datasets where rs62263260 or its neighboring SNPs were significant eQTLs for *SEMA5B*, colocalization results were negative (PP3 > 80%) or inconclusive (**Supplementary Table 7**).

In addition, rs62263260 and SNPs in the surrounding region significantly disrupted 6 transcription factor binding sites (p.fdr<0.05, **Supplementary Table 14**), but were not enriched for enhancer sites and were not methylation-QTLs or histone-QTLs in any queried database.

Post-Hoc Analysis of *SEMA5B* Expression in Brain

Using Agora, a publicly available database powered by the AMP-AD Consortium https://agora.adknowledgeportal.org/genes/(genes-router:gene-details/ENSG00000082684), we examined whether AD diagnosis had any effect on *SEMA5B* gene expression. In multiple brain tissues including cerebellum, prefrontal cortex, and temporal cortex, *SEMA5B* expression is decreased in AD brains in comparison to controls. To ensure that the differences observed on Agora were not due to cell type differences in the bulk tissue, we also leveraged a laser-captured neuronal gene expression dataset[53-56] to assess neuron-specific *SEMA5B* expression differences by diagnosis. Similar to the results seen on Agora, we observed a main effect of diagnosis on *SEMA5B* expression ($F(1, 152)=17.45$, $p < 0.0001$) whereby we observed lower expression of *SEMA5B* in AD compared to control neurons (**Figure 4**). When evaluating each region individually in post-hoc paired comparisons, we observed that the difference was particularly pronounced in the hippocampus ($T(20.768)=-2.79$, $p=0.006$).

Gene and Pathway Results

In gene level analyses, the *TOMM40* interaction with CSF Aβ42 on hippocampal atrophy was the top result ($p=1.60 \times 10^{-5}$, p.fdr=0.28), but did not survive multiple corrections. The *TOMM40* signal was further attenuated when covarying for *APOE* as expected (p.fdr=0.74).[59]

Our top pathway-level results included the GO term "regulation of double strand break repair" ($p=3.11 \times 10^{-4}$) but it did not survive correction. Nominally significant gene- and pathway-level results are reported in **Figure 5** and **Supplementary Tables 15-18.**

DISCUSSION

In the current study, we identified a novel locus that modifies the association between baseline CSF Aβ42 and the annual rate of hippocampal volume decline. Specifically, minor allele (T) carriers of rs62263260 exhibit faster rates of hippocampal atrophy among individuals with biomarker evidence of amyloidosis. In contrast, rs62263260 minor allele carriers with low amyloid burden appear to be protected from neurodegeneration compared to non-carriers. Importantly, we observed evidence of this interaction effect across PET and CSF measures of amyloidosis and replicated this interaction effect in an independent dataset. Moreover, our top variant is a strong eQTL for *SEMA5B*, a gene involved in synaptic pruning and axonal guidance. Additionally, we replicated previous work demonstrating that *APOE*-ε4 modifies the association between baseline CSF amyloid on both cross-sectional and longitudinal measures of hippocampal volume. Though additional studies are needed, the present results suggest that axonal guidance and synaptic pruning genes, along with *APOE,* may modulate the association between amyloid pathology and downstream neurodegeneration, providing exciting targets for future mechanistic studies.

Variants on chromosome 3 drive increased susceptibility to amyloid-dependent neurodegeneration

Notably, our top GWAS finding rs62263260 and the additional SNPs within the region have not been linked to Alzheimer's in any previous case-control studies of clinical Alzheimer's disease and Alzheimer's risk.[60, 61] It is also not significantly associated with diagnosis in our study (p=0.47). As in previous studies examining Alzheimer's disease endophenotypes as outcomes,[62] rs62263260 may be more related to the rate of disease progression than risk for the onset of clinical disease.

rs62263260 is a significant eQTL for the *SEMA5B* gene in two independent eQTL studies and is colocalized with *SEMA5B* in esophageal tissue. Though *SEMA5B* expression in esophageal tissue is not

directly linked to neurodegeneration, it should be noted that studies leveraging the NIH GTEx portal have suggested that genetic regulation of gene expression is conserved across many tissues,[63, 64] thus, significant results in seemingly non-relevant tissues, such as the esophagus, with increased sample size (and subsequently, statistical power), could still provide insights into hypothetical disease processes. However, further study in highly relevant tissues (*i.e.*, hippocampus) is still needed to conclusively elucidate its role in amyloid-related hippocampal atrophy. *SEMA5B* encodes semaphorin 5B (Sema5B), which is expressed in both the developing and adult hippocampus.[49, 65-67] Proteins within the semaphorin family, including Sema5B, facilitate neural development, axonal growth, and synapse maintenance.[68] Sema5B is being actively studied and is not well-characterized, but *Sema5b* knockout mice exhibit aberrant neuronal branching and axonal pathfinding defects.[69-72] In contrast, overexpression of *Sema5b* in mouse hippocampal neurons resulted in a decrease in synapse number.[65]

The direction of the *SEMA5B* association in the present manuscript is difficult to determine, though preliminary eQTL results suggest that the minor allele of rs62263260 is associated with increased expression of *SEMA5B* in tissues including the brain,[50] esophagus, and testes (**Supplementary Figure 4**). Thus, it may be that higher expression of *SEMA5B* is associated with slower hippocampal atrophy in the absence of amyloidosis, but more rapid neurodegeneration in the presence of amyloid. In contrast to the eQTL direction of effect, there is evidence that *SEMA5B* expression is downregulated in Alzheimer's disease brains as reported by the Agora platform (https://agora.ampadportal.org/genes) and within our post-hoc analyses, further suggesting a change over the course of disease. We hypothesize that *SEMA5B* expression and function may change as Alzheimer's disease progresses, though further mechanistic study of *SEMA5B* in relevant brain tissues is truly needed to confirm its role and function in neurodegeneration.

APOE-ε4 carriers exhibit increased susceptibility to neurodegeneration in presence of amyloidosis

APOE-ε4 is the strongest genetic risk factor for late-onset Alzheimer's disease, causing a 2- to 3-fold increased risk of Alzheimer's among heterozygous *APOE*-ε4 carriers, and up to a 15-fold increased risk among homozygous *APOE*-ε4 carriers.[73, 74] *APOE*-ε4 increases the pathological deposition and aggregation of Aβ in the brain – even in cognitively normal older adults – and has also shown evidence of independent associations with tau and cerebrovascular disease.[75, 76] Our analyses add to existing literature suggesting that carriers of *APOE*-ε4 exhibit faster hippocampal volume decline in the presence of brain amyloidosis. Interestingly, the cross-sectional effects on baseline hippocampal volume appear to occur in a dose-dependent manner. However, we do not see any difference in the association between higher levels of amyloid and neurodegeneration in *APOE*-ε4 heterozygotes compared to *APOE*-ε4 homozygotes, perhaps suggesting the additional impact of homozygous carriership on hippocampal volume was already present at baseline in these cohort studies. *APOE*-ε4 positivity has been associated with accelerated seeding of amyloid pathology and an earlier onset of amyloid positivity.[77, 78] Furthermore, it has been suggested that the length of amyloid positivity correlates positively with the rate of the future progression of disease.[78] Altogether, the results add to a growing body of literature suggesting that *APOE* contributes to the progression of Alzheimer's disease both upstream and downstream of amyloidosis.

Strengths and Limitations

This study has multiple strengths including the use of harmonized CSF and PET amyloid values in addition to longitudinal neuroimaging data from well-characterized aging studies. We were also able to replicate our amyloid results in an independent cohort. In this study, as well as others, we have also

demonstrated that our harmonization processes are viable for increasing sample size, laying the foundation for future large-scale genomic discovery analyses of resilience.

However, our study is not without limitations. Our sample was restricted to individuals who were highly educated, non-Hispanic white, and were free of other health comorbidities, limiting the generalizability of our results to additional populations. Though we were able to harmonize and standardize the CSF Aβ42 values and hippocampal volume measurements across cohorts, subtle differences still remain possible due to differences in age and enrollment criteria (**Supplementary Table 4**). Additionally, as our results are based on cross-sectional amyloid data, we cannot exclude that parts of our findings could be explained by the recent suggestion that *APOE* genotype could be used as a surrogate measure of time with Aβ pathology,[79] *i.e.*, that Aβ-positive *APOE*-ε4 carriers have had Aβ pathology 10-15 years longer than Aβ-positive non-carriers, and that they therefore are further along in the neurodegenerative phase of Alzheimer's disease. This hypothesis needs to be addressed in future longitudinal studies.

Looking forward, further efforts to harmonize biomarker and neuroimaging data from additional cohorts will be needed to fully characterize the roles of the newly identified locus in neuroprotection from amyloid pathology.

Conclusion

In this study, we identified a locus on chromosome 3 that modifies the association between baseline CSF amyloid levels and hippocampal atrophy, which our colleagues were able to replicate independently. We also supported previous findings that *APOE*-ε4 increases risk for Alzheimer's disease both upstream and downstream of amyloid pathology. Our results suggest that genes in the axonal branching and synaptic maintenance, along with *APOE*, may be implicated in the downstream consequences of amyloidosis.

ACKNOWLEDGEMENTS

The results published here are in whole or in part based on data obtained from Agora, a platform initially developed by the National Institute on Aging-funded AMP-AD consortium that shares evidence in support of Alzheimer's disease target discovery. In addition, data collection and sharing for this project was funded by the Alzheimer's Disease Neuroimaging Initiative and the Vanderbilt Memory & Alzheimer's Center. Funding details are provided in the Funding section below. The graphical abstract was created with BioRender.com.

FUNDING

This research was supported in part by grants K01-AG049164, K24-AG046373, R01-AG059716, R01-AG034962, R01-HL111516, R01-NS100980, R01-AG056534, R01-AG027161, R01-AG054047, R01-AG021155, R01-AG037639, U01-AG46152, U01-AG006781, U01-AG032984, U01-HG004610, U01-HG006375, U19-AG033655, U24-AG021886, and U24-AG041689 from the Intramural Research Program, the National Institute on Aging, the National Institutes of Health, the Vanderbilt University Advanced Computing Center for Research and Education (ACCRE) instrumentation grant (S10-OD023680), the Vanderbilt Institute for Clinical and Translational Research (VICTR) grant (UL1-TR000445, UL1-TR002243), and the Vanderbilt Memory & Alzheimer's Center. Dr. Deming is supported by the National Institute on Aging T32AG000213 Biology of Aging and Age-Related Disease training grant. Dr. Zetterberg is a Wallenberg Scholar supported by grants from the Swedish Research Council (#2018-02532), the European Research Council (#681712), Swedish State Support for Clinical Research (#ALFGBG-720931), the Alzheimer's Drug Discovery Foundation, USA (#201809-2016862), and the UK Dementia Research Institute at University College London. Dr. Blennow is supported by the Swedish Research Council (#2017-00915), the Alzheimer Drug Discovery Foundation, USA (#RDAPB-201809-2016615), the Swedish Alzheimer Foundation (#AF-742881), Hjärnfonden, Sweden (#FO2017-0243), the Swedish state under

the agreement between the Swedish government and the County Councils, the ALF-agreement (#ALFGBG-715986), and European Union Joint Program for Neurodegenerative Disorders (JPND2019-466-236). Work with the MCSA data was supported by National Institutes of Health grants U01-AG006786, R01-NS097495, R01-AG56366, P50-AG016574, P30-AG062677, R37-AG011378, R01-AG041851, R01-AG034676 and the GHR Foundation. Data collection and sharing for ADNI were supported by National Institutes of Health Grant U01-AG024904 and Department of Defense (award number W81XWH-12-2-0012). ADNI is also funded by the National Institute on Aging, the National Institute of Biomedical Imaging and Bioengineering, and through generous contributions from the following: AbbVie, Alzheimer's Association; Alzheimer's Drug Discovery Foundation; Araclon Biotech; BioClinica, Inc.; Biogen; Bristol-Myers Squibb Company; CereSpir, Inc.; Cogstate; Eisai Inc.; Elan Pharmaceuticals, Inc.; Eli Lilly and Company; EuroImmun; F. Hoffmann-La Roche Ltd and its affiliated company Genentech, Inc.; Fujirebio; GE Healthcare; IXICO Ltd.; Janssen Alzheimer Immunotherapy Research & Development, LLC.; Johnson & Johnson Pharmaceutical Research & Development LLC.; Lumosity; Lundbeck; Merck & Co., Inc.; Meso Scale Diagnostics, LLC.; NeuroRx Research; Neurotrack Technologies; Novartis Pharmaceuticals Corporation; Pfizer Inc.; Piramal Imaging; Servier; Takeda Pharmaceutical Company; and Transition Therapeutics. The Canadian Institutes of Health Research is providing funds to support ADNI clinical sites in Canada. Private sector contributions are facilitated by the Foundation for the National Institutes of Health (www.fnih.org). The grantee organization is the Northern California Institute for Research and Education, and the study is coordinated by the Alzheimer's Therapeutic Research Institute at the University of Southern California. ADNI data are disseminated by the Laboratory for Neuro Imaging at the University of Southern California.

COMPETING INTERESTS

Dr. Zetterberg has served at scientific advisory boards for Denali, Roche Diagnostics, Wave, Samumed, Siemens Healthineers, Pinteon Therapeutics and CogRx, has given lectures in symposia sponsored by Fujirebio, Alzecure and Biogen, and is a co-founder of Brain Biomarker Solutions in Gothenburg AB (BBS), which is a part of the GU Ventures Incubator Program (outside submitted work). Dr. Blennow has served as a consultant, at advisory boards, or at data monitoring committees for Abcam, Axon, Biogen, JOMDD/Shimadzu. Julius Clinical, Lilly, MagQu, Novartis, Roche Diagnostics, and Siemens Healthineers, and is a co-founder of Brain Biomarker Solutions in Gothenburg AB (BBS), which is a part of the GU Ventures Incubator Program. Dr. Johnson serves as a consultant to Roche Diagnostics. Dr. Vemuri has received speaking fees from Miller Medical Communications, LLC. No other authors of this paper have any conflicts of interest to disclose.

SUPPLEMENTARY MATERIAL

Supplementary information is available at *Brain Communications*.

REFERENCES

1. Mehta D, Jackson R, Paul G, Shi J, Sabbagh M. Why do trials for Alzheimer's disease drugs keep failing? A discontinued drug perspective for 2010-2015. *Expert Opin Investig Drugs*. 2017;26(6):735-739. doi:10.1080/13543784.2017.1323868

2. Cummings J. Lessons learned from Alzheimer disease: clinical trials with negative outcomes. *Clinical Translational Science*. 2018;11(2):147-152.

3. Cummings J, Lee G, Ritter A, Sabbagh M, Zhong K. Alzheimer's disease drug development pipeline: 2019. *Alzheimers Dement (N Y)*. 2019;5:272-293. doi:10.1016/j.trci.2019.05.008

4. Cummings JL, Morstorf T, Zhong K. Alzheimer's disease drug-development pipeline: few candidates, frequent failures. *Alzheimer's Research & Therapy*. 2014/07/03 2014;6(4):37. doi:10.1186/alzrt269

5. Driscoll I, Troncoso J. Asymptomatic Alzheimers Disease: A Prodrome or a State of Resilience? *Current Alzheimer Research*. 2011;8(4):330-335.

6. Rahimi J, Kovacs GG. Prevalence of mixed pathologies in the aging brain. *Alzheimers Research & Therapy*. 2014;6(9):82.

7. Sonnen JA, Santa Cruz K, Hemmy LS, et al. Ecology of the aging human brain. *Archives of Neurology*. 2011;68(8):1049-1056.

8. Stern Y. Cognitive reserve in ageing and Alzheimer's disease. *The Lancet Neurology*. 2012;11(11):1006-1012. doi:10.1016/S1474-4422(12)70191-6

9. Hohman TJ, McLaren DG, Mormino EC, Gifford KA, Libon DJ, Jefferson AL. Asymptomatic Alzheimer disease: Defining resilience. *Neurology*. 2016;87(23):2443-2450.

10. Snowdon DA, Kemper SJ, Mortimer JA, Greiner LH, Wekstein DR, Markesbery WR. Linguistic Ability in Early Life and Cognitive Function and Alzheimer's Disease in Late Life: Findings From the Nun Study. *JAMA*. 1996;275(7):528-532. doi:10.1001/jama.1996.03530310034029

11. Snowdon DA. Aging and Alzheimer's disease: lessons from the Nun Study. *Gerontologist*. Apr 1997;37(2):150-6. doi:10.1093/geront/37.2.150

12. Hohman TJ, Bell SP, Jefferson AL. The Role of Vascular Endothelial Growth Factor in Neurodegeneration and Cognitive Decline: Exploring Interactions With Biomarkers of Alzheimer Disease. *JAMA Neurology*. 2015;72(5):520-529.

13. Hohman TJ, Dumitrescu L, Cox NJ, Jefferson AL. Genetic resilience to amyloid related cognitive decline. *Brain Imaging and Behavior*. 2016:1-9.

14. Mukherjee S, Kim S, Ramanan VK, et al. Gene-based GWAS and biological pathway analysis of the resilience of executive functioning. *Brain Imaging and Behavior*. 2013;8(1):110-118.

15. Teipel SJ. Risk and resilience: a new perspective on Alzheimer's Disease. *Geriatric Mental Health Care*. 2013;1(3):47-55.

16. Arboleda-Velasquez JF, Lopera F, O'Hare M, et al. Resistance to autosomal dominant Alzheimer's disease in an APOE3 Christchurch homozygote: a case report. *Nature Medicine*. 2019/11/01 2019;25(11):1680-1683. doi:10.1038/s41591-019-0611-3

17. Chiang GC, Insel PS, Tosun D, et al. Hippocampal atrophy rates and CSF biomarkers in elderly APOE2 normal subjects. *Neurology*. 2010;75(22):1976-1981. doi:10.1212/WNL.0b013e3181ffe4d1

18. Corder EH, Saunders AM, Risch NJ, et al. Protective effect of apolipoprotein E type 2 allele for late onset Alzheimer disease. *Nature Genetics*. 1994/06/01 1994;7(2):180-184. doi:10.1038/ng0694-180

19. Safieh M, Korczyn AD, Michaelson DM. ApoE4: an emerging therapeutic target for Alzheimer's disease. *BMC Medicine*. 2019/03/20 2019;17(1):64. doi:10.1186/s12916-019-1299-4

20. Dumitrescu L, Mahoney ER, Mukherjee S, et al. Genetic variants and functional pathways associated with resilience to Alzheimer's disease. *Brain*. Aug 1 2020;143(8):2561-2575. doi:10.1093/brain/awaa209

21. Jack CR, Jr., Bennett DA, Blennow K, et al. NIA-AA Research Framework: Toward a biological definition of Alzheimer's disease. *Alzheimers Dement*. Apr 2018;14(4):535-562. doi:10.1016/j.jalz.2018.02.018

22. Jack CR, Knopman DS, Jagust WJ, et al. Hypothetical model of dynamic biomarkers of the Alzheimer's pathological cascade. *The Lancet Neurology*. 2010;9(1):119.

23. Jack CR, Knopman DS, Jagust WJ, et al. Tracking pathophysiological processes in Alzheimer's disease: an updated hypothetical model of dynamic biomarkers. *The Lancet Neurology*. 2013;12(2):207-216.

24. Stricker NH, Dodge HH, Dowling NM, Han SD, Erosheva EA, Jagust WJ. CSF biomarker associations with change in hippocampal volume and precuneus thickness: implications for the Alzheimer's pathological cascade. *Brain Imaging and Behavior*. 2012;6(4):599-609.

25. Andrews KA, Frost C, Modat M, et al. Acceleration of hippocampal atrophy rates in asymptomatic amyloidosis. *Neurobiology of Aging*. 2016/03/01/ 2016;39:99-107. doi:https://doi.org/10.1016/j.neurobiolaging.2015.10.013

26. Fletcher E, Villeneuve S, Maillard P, et al. β-amyloid, hippocampal atrophy and their relation to longitudinal brain change in cognitively normal individuals. *Neurobiology of aging*. 2016;40:173-180. doi:10.1016/j.neurobiolaging.2016.01.133

27. Frankó E, Joly O, for the Alzheimer's Disease Neuroimaging I. Evaluating Alzheimer's Disease Progression Using Rate of Regional Hippocampal Atrophy. *PLOS ONE*. 2013;8(8):e71354. doi:10.1371/journal.pone.0071354

28. Purcell S, Neale B, Todd-Brown K, et al. PLINK: a tool set for whole-genome association and population-based linkage analyses. *The American Journal of Human Genetics*. 2007;81(3):559-575.

29. Price AL, Patterson NJ, Plenge RM, Weinblatt ME, Shadick NA, Reich D. Principal components analysis corrects for stratification in genome-wide association studies. *Nature genetics*. 2006;38(8):904-909.

30. Das S, Forer L, Schonherr S, et al. Next-generation genotype imputation service and methods. *Nat Genet*. Oct 2016;48(10):1284-1287. doi:10.1038/ng.3656

31. Ramanan VK, Lesnick TG, Przybelski SA, et al. Coping with brain amyloid: genetic heterogeneity and cognitive resilience to Alzheimer's pathophysiology. *Acta Neuropathol Commun*. Mar 23 2021;9(1):48. doi:10.1186/s40478-021-01154-1

32. Pettigrew C, Soldan A, Zhu Y, et al. Cognitive reserve and cortical thickness in preclinical Alzheimer's disease. *Brain Imaging Behav*. 2017;11(2):357-367. doi:10.1007/s11682-016-9581-y

33. Jefferson AL, Gifford KA, Acosta LMY, et al. The Vanderbilt Memory & Aging Project: Study Design and Baseline Cohort Overview. *Journal of Alzheimer's Disease*. 2016;(Preprint):1-20.

34. Johnson SC, Koscik RL, Jonaitis EM, et al. The Wisconsin Registry for Alzheimer's Prevention: A review of findings and current directions. *Alzheimer & Dementia: DADM*. 2018;10:130-142. doi:10.1016/j.dadm.2017.11.007

35. About ADNI. 2008. http://www.adni-info.org/Scientists/AboutADNI.aspx

36. Whitwell JL, Wiste HJ, Weigand SD, et al. Comparison of imaging biomarkers in the Alzheimer Disease Neuroimaging Initiative and the Mayo Clinic Study of Aging. *Arch Neurol*. 2012;69(5):614-622. doi:10.1001/archneurol.2011.3029

37. Varatharajah Y, Ramanan VK, Iyer R, Vemuri P. Predicting Short-term MCI-to-AD Progression Using Imaging, CSF, Genetic Factors, Cognitive Resilience, and Demographics. *Sci Rep*. Feb 19 2019;9(1):2235. doi:10.1038/s41598-019-38793-3

38. Jack CR, Jr., Bernstein MA, Fox NC, et al. The Alzheimer's Disease Neuroimaging Initiative (ADNI): MRI methods. *J Magn Reson Imaging*. Apr 2008;27(4):685-91. doi:10.1002/jmri.21049

39. Wennberg AMV, Lesnick TG, Schwarz CG, et al. Longitudinal Association Between Brain Amyloid-Beta and Gait in the Mayo Clinic Study of Aging. *The Journals of Gerontology: Series A*. 2018;73(9):1244-1250. doi:10.1093/gerona/glx240

40. Moghekar A, Li S, Lu Y, et al. CSF biomarker changes precede symptom onset of mild cognitive impairment. *Neurology*. November 12, 2013 2013;81(20):1753-1758. doi:10.1212/01.wnl.0000435558.98447.17

41. Mormino EC, Betensky RA, Hedden T, et al. Amyloid and APOE ε4 interact to influence short-term decline in preclinical Alzheimer disease. *Neurology*. 2014;82(20):1760-1767.

42. Raghavan NS, Dumitrescu L, Mormino E, et al. Common Variants in RBFOX1 are Associated with Brain Amyloidosis. *In Review*. 2020;

43. Deming Y, Li Z, Kapoor M, et al. Genome-wide association study identifies four novel loci associated with Alzheimer's endophenotypes and disease modifiers. *Acta Neuropathologica*. May 2017;133(5):839-856. doi:10.1007/s00401-017-1685-y

44. Ramanan VK, Wang X, Przybelski SA, et al. Variants in PPP2R2B and IGF2BP3 are associated with higher tau deposition. *Brain Communications*. 2020;2(2)doi:10.1093/braincomms/fcaa159

45. Jack CR, Jr., Wiste HJ, Weigand SD, et al. Defining imaging biomarker cut points for brain aging and Alzheimer's disease. *Alzheimers Dement*. Mar 2017;13(3):205-216. doi:10.1016/j.jalz.2016.08.005

46. Properzi MJ, Buckley RF, Chhatwal JP, et al. Nonlinear Distributional Mapping (NoDiM) for harmonization across amyloid-PET radiotracers. *Neuroimage*. Feb 1 2019;186:446-454. doi:10.1016/j.neuroimage.2018.11.019

47. Roostaei T, Nazeri A, Felsky D, et al. Genome-wide interaction study of brain beta-amyloid burden and cognitive impairment in Alzheimer's disease. *Mol Psychiatry*. Feb 2017;22(2):287-295. doi:10.1038/mp.2016.35

48. Raghavan NS, Dumitrescu L, Mormino E, et al. Association Between Common Variants in RBFOX1, an RNA-Binding Protein, and Brain Amyloidosis in Early and Preclinical Alzheimer Disease. *JAMA Neurol*. Jun 22 2020;doi:10.1001/jamaneurol.2020.1760

49. Lonsdale J, Thomas J, Salvatore M, et al. The Genotype-Tissue Expression (GTEx) project. Commentary. *Nature Genetics*. 06//print 2013;45(6):580-585. doi:10.1038/ng.2653 http://www.nature.com/ng/journal/v45/n6/abs/ng.2653.html#supplementary-information

50. Sieberts SK, Perumal TM, Carrasquillo MM, et al. Large eQTL meta-analysis reveals differing patterns between cerebral cortical and cerebellar brain regions. *Scientific Data*. 2020/10/12 2020;7(1):340. doi:10.1038/s41597-020-00642-8

51. Wallace C. Eliciting priors and relaxing the single causal variant assumption in colocalisation analyses. *PLOS Genetics*. 2020;16(4):e1008720. doi:10.1371/journal.pgen.1008720

52. Giambartolomei C, Vukcevic D, Schadt EE, et al. Bayesian Test for Colocalisation between Pairs of Genetic Association Studies Using Summary Statistics. *PLOS Genetics*. 2014;10(5):e1004383. doi:10.1371/journal.pgen.1004383

53. Liang WS, Dunckley T, Beach TG, et al. Gene expression profiles in anatomically and functionally distinct regions of the normal aged human brain. *Physiol Genomics*. 2007;28(3):311-322. doi:10.1152/physiolgenomics.00208.2006

54. Readhead B, Haure-Mirande JV, Funk CC, et al. Multiscale Analysis of Independent Alzheimer's Cohorts Finds Disruption of Molecular, Genetic, and Clinical Networks by Human Herpesvirus. *Neuron*. Jul 11 2018;99(1):64-82.e7. doi:10.1016/j.neuron.2018.05.023

55. Liang WS, Dunckley T, Beach TG, et al. Altered neuronal gene expression in brain regions differentially affected by Alzheimer's disease: a reference data set. *Physiol Genomics*. Apr 22 2008;33(2):240-56. doi:10.1152/physiolgenomics.00242.2007

56. Liang WS, Reiman EM, Valla J, et al. Alzheimer's disease is associated with reduced expression of energy metabolism genes in posterior cingulate neurons. *Proc Natl Acad Sci U S A*. Mar 18 2008;105(11):4441-6. doi:10.1073/pnas.0709259105

57. de Leeuw CA, Mooij JM, Heskes T, Posthuma D. MAGMA: generalized gene-set analysis of GWAS data. *PLoS Comput Biol*. 2015;11(4):e1004219-e1004219. doi:10.1371/journal.pcbi.1004219

58. Chiang GC, Insel PS, Tosun D, et al. Impact of apolipoprotein E4-cerebrospinal fluid β-amyloid interaction on hippocampal volume loss over 1 year in mild cognitive impairment. *Alzheimer's & dementia : the journal of the Alzheimer's Association*. 2011;7(5):514-520. doi:10.1016/j.jalz.2010.12.010

59. Yu C-E, Seltman H, Peskind ER, et al. Comprehensive analysis of APOE and selected proximate markers for late-onset Alzheimer's disease: patterns of linkage disequilibrium and disease/marker association. *Genomics*. 2007;89(6):655-665. doi:10.1016/j.ygeno.2007.02.002

60. Kunkle BW, Grenier-Boley B, Sims R, et al. Genetic meta-analysis of diagnosed Alzheimer’s disease identifies new risk loci and implicates Aβ, tau, immunity and lipid processing. *Nature Genetics*. 2019/03/01 2019;51(3):414-430. doi:10.1038/s41588-019-0358-2

61. Jansen IE, Savage JE, Watanabe K, et al. Genome-wide meta-analysis identifies new loci and functional pathways influencing Alzheimer’s disease risk. *Nature Genetics*. 2019/03/01 2019;51(3):404-413. doi:10.1038/s41588-018-0311-9

62. Cruchaga C, Kauwe JSK, Mayo K, et al. SNPs associated with cerebrospinal fluid phospho-tau levels influence rate of decline in Alzheimer's disease. *PLoS Genetics*. 2010;6(9):e1001101.

63. Bahcall OG. GTEx pilot quantifies eQTL variation across tissues and individuals. *Nature Reviews Genetics*. 2015/07/01 2015;16(7):375-375. doi:10.1038/nrg3969

64. Aguet F, Brown AA, Castel SE, et al. Genetic effects on gene expression across human tissues. *Nature*. 2017/10/01 2017;550(7675):204-213. doi:10.1038/nature24277

65. O'Connor TP, Cockburn K, Wang W, Tapia L, Currie E, Bamji SX. Semaphorin 5B mediates synapse elimination in hippocampal neurons. *Neural Development*. 2009/05/23 2009;4(1):18. doi:10.1186/1749-8104-4-18

66. Zhang Y, Chen K, Sloan SA, et al. An RNA-Sequencing Transcriptome and Splicing Database of Glia, Neurons, and Vascular Cells of the Cerebral Cortex. *The Journal of Neuroscience*. 2014;34(36):11929. doi:10.1523/JNEUROSCI.1860-14.2014

67. Zhang Y, Sloan Steven A, Clarke Laura E, et al. Purification and Characterization of Progenitor and Mature Human Astrocytes Reveals Transcriptional and Functional Differences with Mouse. *Neuron*. 2016;89(1):37-53. doi:10.1016/j.neuron.2015.11.013

68. Alto LT, Terman JR. Semaphorins and their Signaling Mechanisms. *Methods in molecular biology (Clifton, NJ)*. 2017;1493:1-25. doi:10.1007/978-1-4939-6448-2_1

69. Jung JS, Zhang KD, Wang Z, et al. Semaphorin-5B Controls Spiral Ganglion Neuron Branch Refinement during Development. *The Journal of Neuroscience*. 2019;39(33):6425. doi:10.1523/JNEUROSCI.0113-19.2019

70. Lett RLM, Wang W, O'Connor TP. Semaphorin 5B Is a Novel Inhibitory Cue for Corticofugal Axons. *Cerebral Cortex*. 2008;19(6):1408-1421. doi:10.1093/cercor/bhn179

71. Liu RQ, Wang W, Legg A, Abramyan J, Connor TP. Semaphorin 5B is a repellent cue for sensory afferents projecting into the developing spinal cord. *Development*. 2014;141(9):1940. doi:10.1242/dev.103630

72. Matsuoka RL, Chivatakarn O, Badea TC, et al. Class 5 transmembrane semaphorins control selective Mammalian retinal lamination and function. *Neuron*. 2011;71(3):460-473. doi:10.1016/j.neuron.2011.06.009

73. Liu C-C, Kanekiyo T, Xu H, Bu G. Apolipoprotein E and Alzheimer disease: risk, mechanisms and therapy. 10.1038/nrneurol.2012.263. *Nature Reviews Neurology*. 02//print 2013;9(2):106-118.

74. Reiman EM, Arboleda-Velasquez JF, Quiroz YT, et al. Exceptionally low likelihood of Alzheimer's dementia in APOE2 homozygotes from a 5,000-person neuropathological study. *Nature Communications*. 2020/02/03 2020;11(1):667. doi:10.1038/s41467-019-14279-8

75. Shi Y, Yamada K, Liddelow SA, et al. ApoE4 markedly exacerbates tau-mediated neurodegeneration in a mouse model of tauopathy. *Nature*. 2017;549(7673):523-527.

76. Yip AG, McKee AC, Green RC, et al. APOE, vascular pathology, and the AD brain. *Neurology*. Jul 26 2005;65(2):259-65. doi:10.1212/01.wnl.0000168863.49053.4d

77. Yamazaki Y, Zhao N, Caulfield TR, Liu C-C, Bu G. Apolipoprotein E and Alzheimer disease: pathobiology and targeting strategies. *Nature Reviews Neurology*. 2019/09/01 2019;15(9):501-518. doi:10.1038/s41582-019-0228-7

78. Koscik RL, Betthauser TJ, Jonaitis EM, et al. Amyloid duration is associated with preclinical cognitive decline and tau PET. *Alzheimer's & Dementia: Diagnosis, Assessment & Disease Monitoring*. 2020/01/01 2020;12(1):e12007. doi:10.1002/dad2.12007

79. Lautner R, Insel PS, Skillbäck T, et al. Preclinical effects of APOE ε4 on cerebrospinal fluid Aβ42 concentrations. *Alzheimers Res Ther*. Oct 23 2017;9(1):87. doi:10.1186/s13195-017-0313-3

Table 1. Participant characteristics by diagnosis

	NC	MCI	AD	Total[a]	p-value
N	490	475	100	1065	
Age at baseline	68.4±9.3	72.5±7.3	74.5±8.4	70.8±8.7	< 0.001
Sex, % female	53%	39%	48%	47%	0.002
% *APOE*-ε4 carriers	29%	47%	67%	41%	< 0.001
% *APOE*-ε2 carriers	13%	9%	3%	10%	< 0.001
Std. CSF Aβ42	-0.75±1.6	-1.70±1.7	-2.52±1.3	-1.34±1.7	< 0.001
Number of Visits	3.46±1.83	4.00±1.86	2.80±1.22	3.64±1.83	0.9
Neuroimaging Measurements (MRI)					
Std. Hippocampal Volume	-0.01±1.0	-0.84±1.3	-2.1±1.3	-0.58±1.3	< 0.001
Std. Hippocampal Vol. Slopes	-0.10±0.1	-0.15±0.1	0.21±0.1	-0.14±0.1	< 0.001

Analysis of variance (ANOVA) analyses indicated significant differences ($p<0.05$) across diagnostic groups for all demographic categories except for the average number of visits. Values given are mean ± standard deviation unless otherwise noted.

[a]Consists of participants from ADNI, VMAP, WRAP, and BIOCARD.

Abbreviations: NC, normal cognition; MCI, mild cognitive impairment, AD, Alzheimer's disease; CSF, cerebrospinal fluid; Aβ-42, β-amyloid-42

Table 2. *APOE*-ε4 and *APOE*-ε2 associations with baseline hippocampal volume

Predictor	Outcome	B	SE	P value	Adj. r^2	Δr^2
APOE-ε4[a]	Baseline HV	-0.43	0.05	< 2.00e-16	0.185	0
APOE-ε4 x CSF Aβ42[b]	Baseline HV	0.11	0.03	0.0004	0.216	3.1
APOE-ε2[a]	Baseline HV	0.25	0.10	0.0168	0.146	0
APOE-ε2 x CSF Aβ42[b]	Baseline HV	-0.13	0.06	0.0435	0.201	5.5
APOE-ε4[a]	Longitudinal HV	-0.031	0.003	< 2.00e-16	0.193	0
APOE-ε4 x CSF Aβ42[b]	Longitudinal HV	0.0056	0.002	0.0024	0.248	5.5
APOE-ε2[a]	Longitudinal HV	0.0236	0.006	0.0002	0.140	0
APOE-ε2 x CSF Aβ42[b]	Longitudinal HV	-0.0054	0.004	0.152	0.235	9.5

[a] Model: Hippocampal Volume ~ Age + Sex + ***APOE***

[b] Model: Hippocampal Volume ~ Age + Sex + ***APOE* x CSF Aβ-42**

Abbreviations: HV, hippocampal volume; B, beta; SE, standard error; Δr^2; change in r^2; Adj. r^2, adjusted r^2

Table 3. Variant Interactions with CSF β-Amyloid

variant	chromosome	BP	allele	MAF	B	SE	P value
rs62263260	3	122675327	T	0.121	0.02621	0.0046	1.46e-08
rs11707826	3	122676305	T	0.122	0.02616	0.0046	1.53e-08
rs10934626	3	122676523	T	0.122	0.02616	0.0046	1.53e-08

Abbreviations: BP, base pair, MAF, minor allele frequency, B, beta; SE, standard error

FIGURE LEGENDS

Fig. 1. *APOE*-ε4 allele carriers have smaller hippocampal volumes at baseline and worse atrophy in the presence of high levels of brain amyloid pathology. A) A plot demonstrating how *APOE*-ε4 allele count modifies the association between Aβ42 and baseline hippocampal volume in a dose-dependent manner (β=0.11, p=0.0004). The y-axis represents baseline standardized hippocampal volume, and the x-axis represents standardized CSF levels of Aβ42 (z-scores). Points and lines are color coded by genotype, where *APOE*-ε4 heterozygotes are denoted by the green line and homozygotes are red. **B)** *APOE*-ε4 positivity increases the rate of atrophy in individuals with high brain amyloid burden (β=0.0056, p=0.0024). There appears to be no change between heterozygous and homozygous carriers of the ε4 allele.

Fig. 2. Three SNPs in an intronic region of the *SEMA5B* gene met genome-wide significance in the SNP x CSF A*β*42 GWAS. A) The Manhattan plot of the genome-wide association study. The threshold for genome-wide statistical significance ($\alpha=5x10^{-8}$) is indicated by the red line. The blue line represents the suggestive threshold for significance ($\alpha=1x10^{-5}$). **B)** A LocusZoom plot of *SEMA5B* and additional genes in the 1Mb region. Points are colored by LD with the top variant, where higher r^2 values are colored in red and lower r^2 values are colored in blue based off of LD calculated in non-Hispanic whites of European descent. The diamond represents the variant with the smallest P-value.

Fig. 3. rs62263260, the index SNP, modifies the association between baseline beta-amyloid and hippocampal atrophy A) A plot demonstrating how the index SNP, rs62263260, modifies the association between CSF Aβ42 and hippocampal atrophy. The y-axis represents annual change in standardized hippocampal volume, and the x-axis represents standardized CSF levels of Aβ42 (z-scores). Points and lines are color coded by genotype. Individuals harboring higher levels of baseline pathology exhibit worse hippocampal atrophy ($\beta=0.026$, $p=1.46x10^{-8}$). **B)** Tissues where rs62263260 or rs10934626 (LD $r^2>0.9$) is a statistically significant eQTL for the *SEMA5B* gene.

Fig. 4. Hippocampal pyramidal neurons in Alzheimer's disease brains express less *SEMA5B* than those from cognitively normal controls. A box plot summarizing laser-captured neuronal expression of *SEMA5B* across brain regions (i.e., entorhinal cortex, hippocampus, medial temporal gyrus, posterior cingulate cortex, primary visual cortex, and superior frontal gyrus) in AD cases and controls such that each point represents a sample's *SEMA5B* expression. Across regions, we observed lower expression of *SEMA5B* in AD compared to controls ($F(1, 152)=17.45$, $p<0.0001$). In post-hoc paired comparisons, the association was particularly pronounced in the hippocampus surviving Bonferroni correction for multiple comparisons (p=0.006).

Fig. 5. Summary of nominally significant MAGMA gene- and pathway-level results. A) A Manhattan plot summarizing chromosome and p-value for all genes tested by MAGMA. The threshold for nominal significance is indicated by the blue line ($\alpha=1x10^{-3}$). *TOMM40* is the most significant result with a p-value of $1.60x10^{-5}$. **B)** A bar plot summarizing pathway-level results with $p < 1x10^{-3}$. The y-axis represents the number of genes in each pathway gene set. Bars are filled according to p-value. The most significant pathway is "regulation of double strand break repair" ($p=3.11x10^{-4}$).

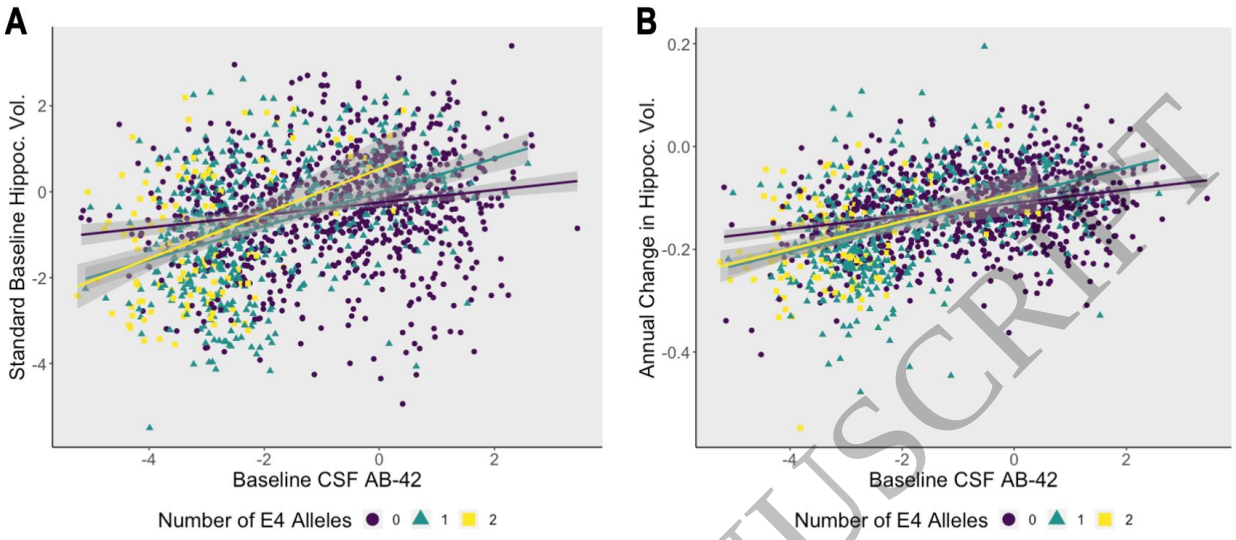

Figure 1
165x75 mm (1.6 x DPI)

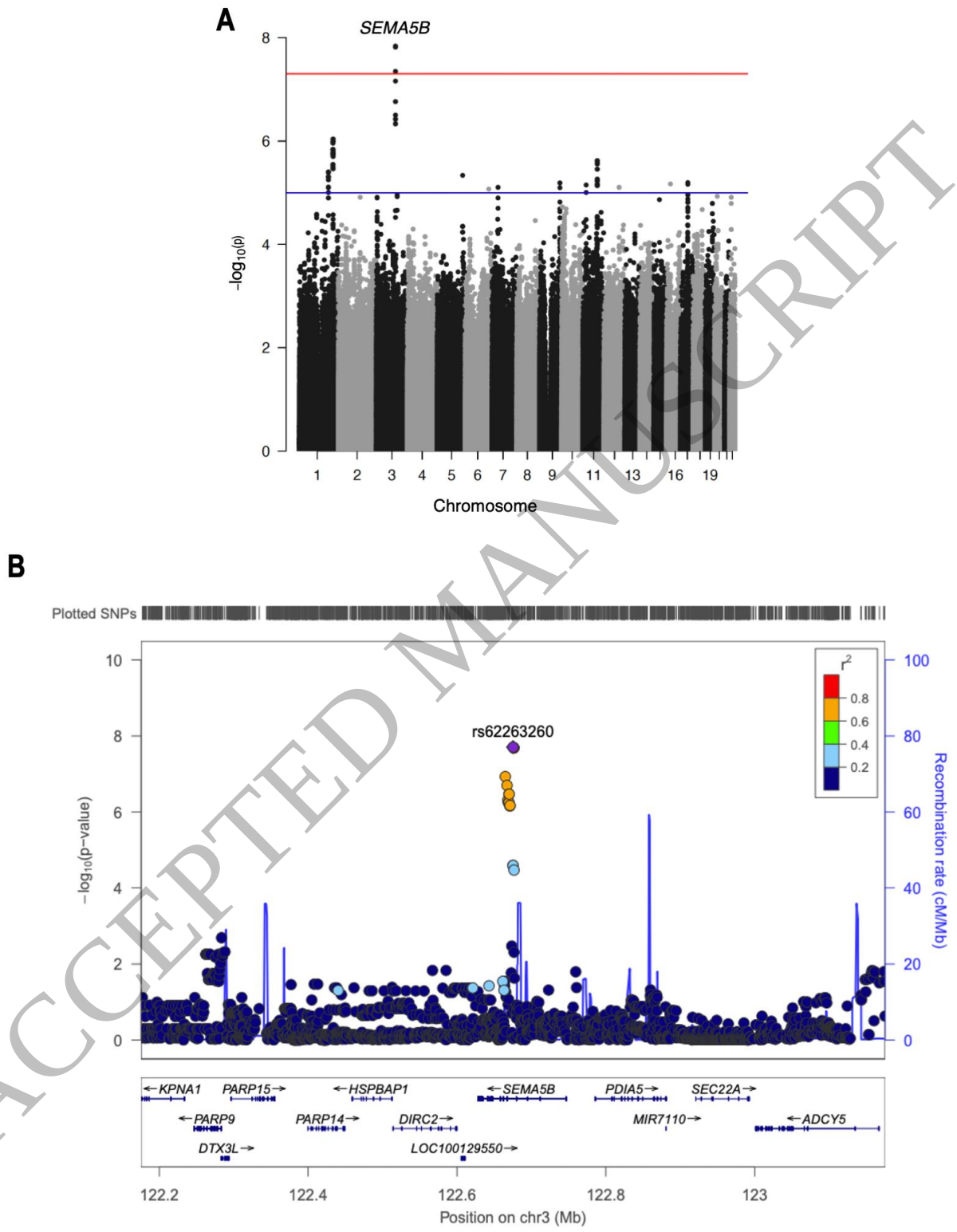

Figure 2
165x213 mm (1.6 x DPI)

1

A

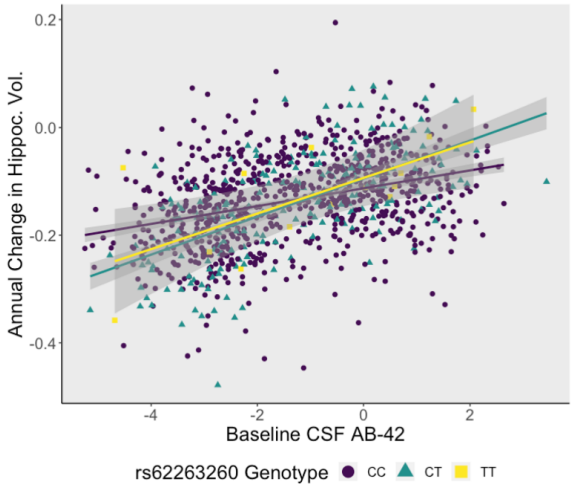

B

Significant eQTLs for rs62263260/rs10934626			
gene	SNP	tissue	P value
SEMA5B	rs62263260	GTEx Esophagus Muscularis	1.9e-6
SEMA5B	rs62263260	GTEx Anterior Cingulate Cortex (BA24)	0.00048
SEMA5B	rs10934626	GTEx Testis	9.5e-5
SEMA5B	rs62263260	AMP-AD Brain Cortex	1.1e-8

2

3 **Figure 3**
4 **165x74 mm (1.6 x DPI)**

5

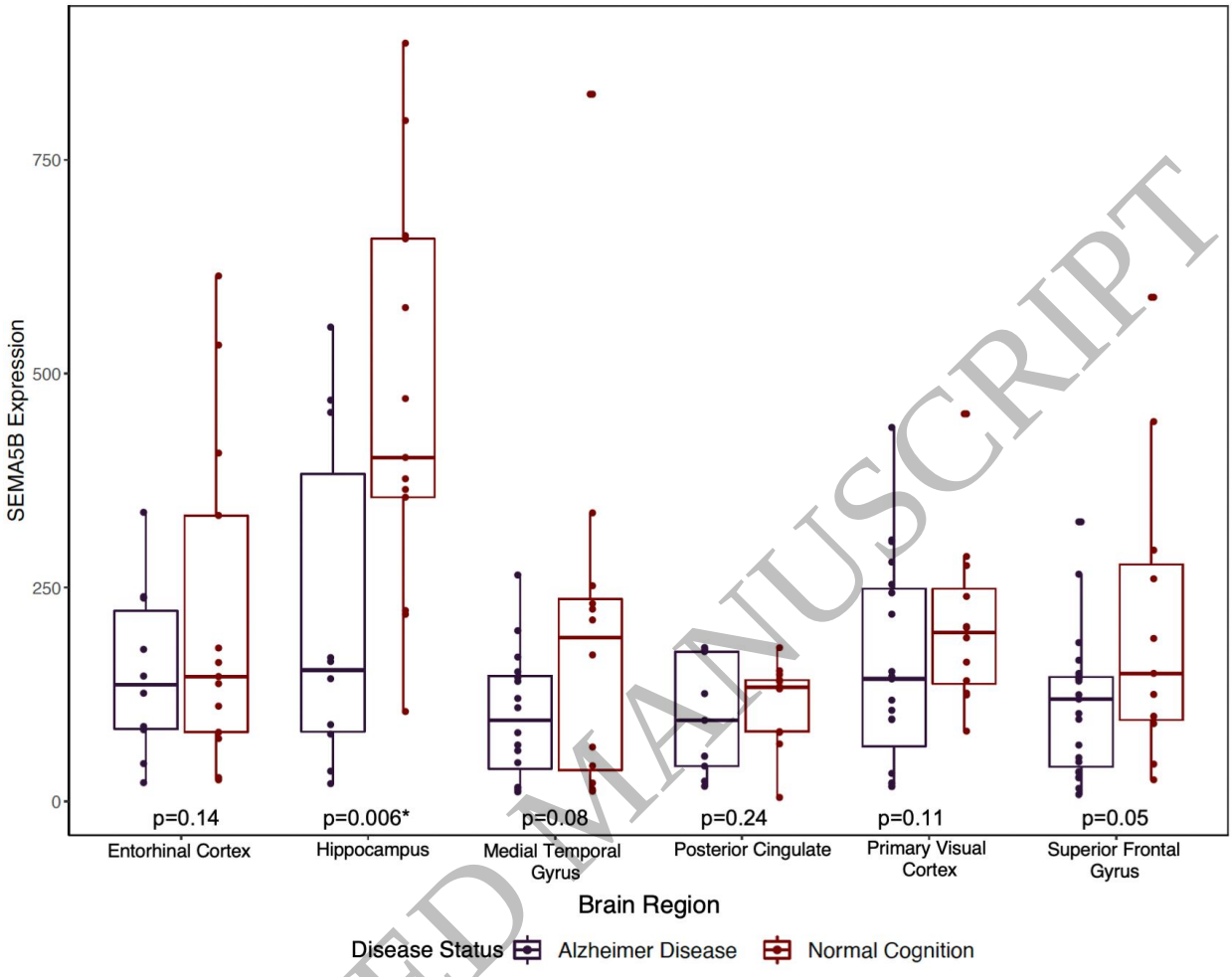

Figure 4
165x133 mm (1.6 x DPI)

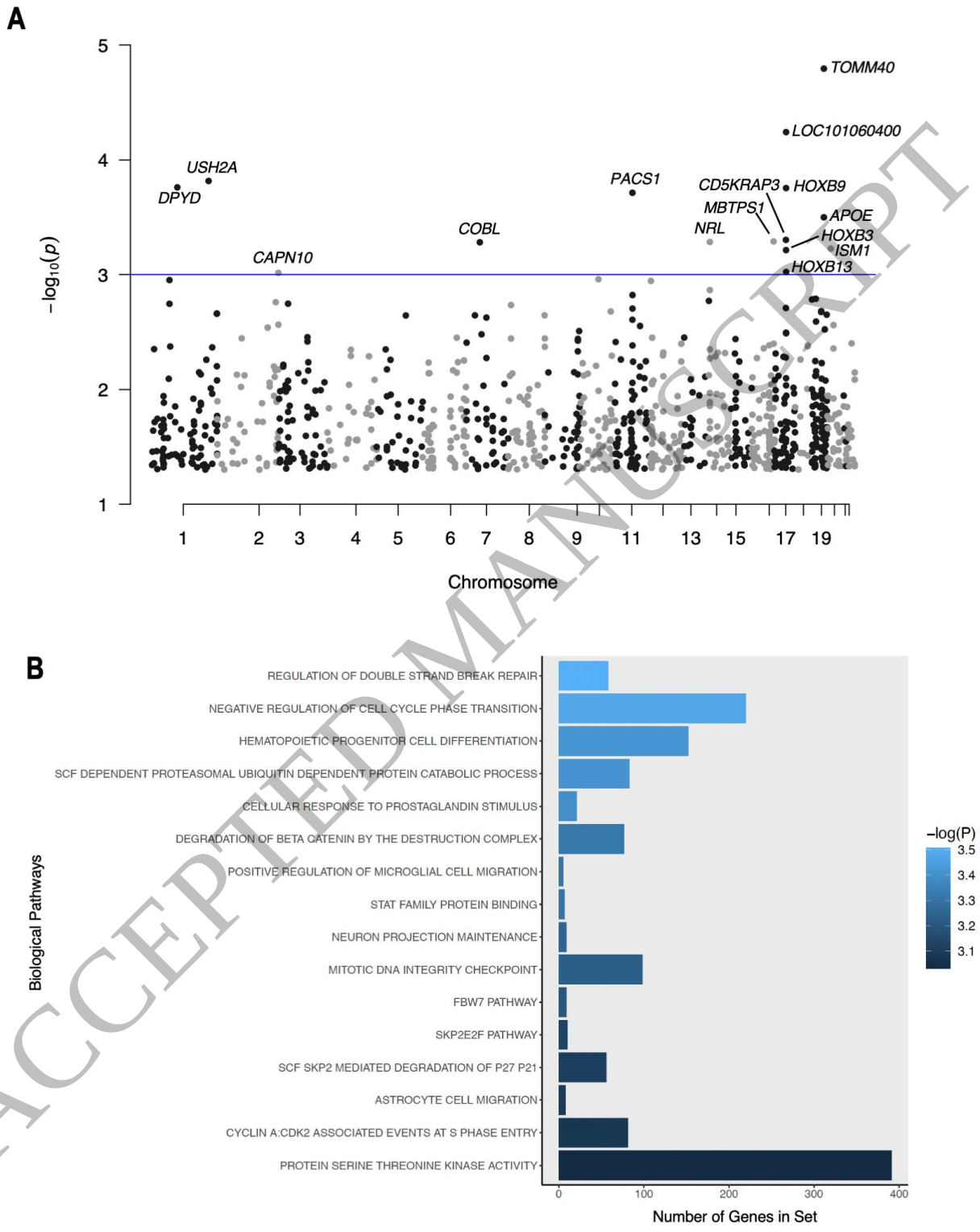

Figure 5
165x208 mm (1.6 x DPI)